

Study of the Production of K X Rays in Ca, Ti, and Ni by 2–28-MeV Protons*

G. A. Bissinger, J. M. Joyce, E. J. Ludwig, W. S. McEver, and S. M. Shafroth

University of North Carolina, Chapel Hill, North Carolina 27514,

and Triangle Universities Nuclear Laboratory, Durham, North Carolina 27706

(Received 24 September 1969)

Using a proportional counter as an x-ray detector, thin-target yields, as well as K x-ray production and ionization cross sections, were determined for Ca, Ti, and Ni when bombarded with 2–28-MeV protons. Broad maxima in the cross sections were found at approximately 8.5, 10.4, and 16.6 MeV for Ca, Ti, and Ni, respectively, in agreement with theoretical calculations based on the Bethe–Born approximation. The shape of the cross-section-versus-bombarding-energy curve agrees well with theory. However, the absolute values of the cross sections were observed to be higher than predicted by theory when the generally accepted value for the effective charge ($Z - 0.3$) was chosen.

I. INTRODUCTION

Measurements of x-ray production cross sections due to bombardment of atoms by baryons have been made sporadically since Chadwick¹ in 1912 first observed and identified characteristic x rays of several elements exposed to α rays. The history of this early work is given in papers by Lewis, Simmons, and Merzbacher² and Merzbacher and Lewis.³ The former authors measured proton induced K x-ray production cross sections 1.7–3 MeV for Mo, Ag, Ta, Au, and Pb, using thick targets and scintillation counter x-ray detectors. They compared their results with the nonrelativistic plane-wave Born-approximation cross-section calculations of Henneberg,⁴ and found general agreement with the trend of the energy dependence of the cross section but found deviations between theory and experiment of up to factors of 4, with the experimental yields being higher than predicted, especially for higher Z targets. Recently, Hart *et al.*⁵ measured oxygen K -shell x-ray production in thin films of aluminum oxide for 20–100-keV protons. They found deviations from the Born-approximation calculations of Merzbacher and Lewis³ at these low energies. At the lowest energies, their experimental data lie below the theoretical curve but they cross the latter at $E_p \approx 500$ keV. Similar results were obtained by Khan, Potter, and Worley⁶ for protons on aluminum.

The present work was primarily designed to see if the K x-ray production cross section, as a function of increasing energy, would rise sharply to a maximum near the energy that corresponds to a proton velocity equaling the rms K -shell electron velocity and then slowly descend as predicted.³ Although expected on very general grounds, to our knowledge this maximum has not previously been observed, except for carbon⁶ and helium.⁷

In the present work, the proton energy range of the cyclo-Graaff (2–30 MeV) and the x-ray de-

tector (a proportional counter) dictated the choice of target elements. In contrast to much of the previous work where thick targets were used,² thin targets were employed for this study. Thus, K x-ray production cross sections at each bombarding energy were determined directly without relying on an integration of a theoretical energy dependence or knowledge of the stopping power. Thin targets had the additional advantage of (i) permitting the x-ray counter to be located closer to the target without being exposed to excessive counting rates, thus reducing the x-ray air-path absorption correction significantly, and (ii) eliminating the necessity for x-ray self-absorption corrections.

A secondary aim of the present work was to determine the absolute values of the x-ray production cross sections. After correcting the x-ray production cross sections for Auger effect, K -shell ionization cross sections are extracted. These can be compared with theory and are useful in testing the so-called shell corrections⁸ in the theory of stopping of heavy charged particles in matter.

II. EXPERIMENT

Characteristic K x rays were produced by bombarding thin targets of Ca, Ti, and Ni with 0.2–15-nA proton beams of from 2–15 MeV supplied by the Triangle Universities Nuclear Laboratory (TUNL) model FN tandem Van de Graaff, and from 15 to 28 MeV with protons from the TUNL cyclo-Graaff⁹ consisting of a 15-MeV fixed-energy isochronous cyclotron injecting a H^- beam into the tandem. A 3-in.-diam gold-plated target chamber was employed after suitable modification for this experiment.¹⁰ A schematic diagram showing the target chamber, x-ray counter, and electronics is shown in Fig. 1.

The Ca and Ti targets were made from the metal evaporated onto thin carbon-foil backings.

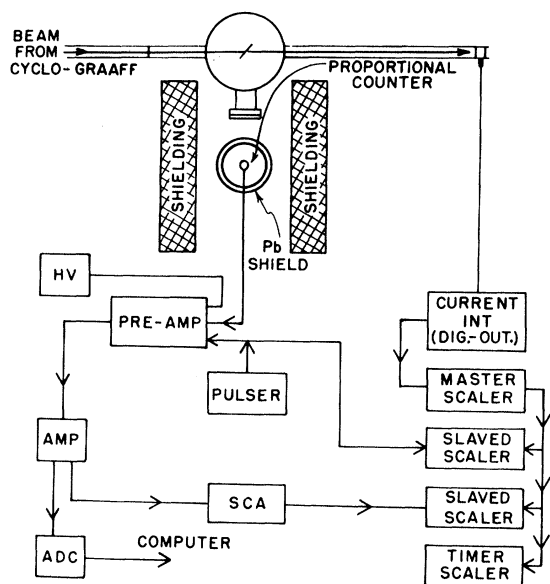


FIG. 1. Schematic diagram of the experimental arrangement.

The target thicknesses were uniform to better than 10%. The Ca was 98% ^{44}Ca , while the titanium was the natural metal. The Ni target¹¹ was supplied in the form of a foil on a Cu backing, which was etched off, producing a self-supporting target, $1.0 \pm 0.2 \times 10^{-5}$ cm thick and uniform to better than 2%, according to the manufacturer.

The target thicknesses were checked by elastic scattering measurements at 30° (lab) with 6.00-MeV α particles. In addition, the thickness of an earlier Ca target (later broken) was measured using 5.00-MeV protons. All measurements were checked for possible deviations from Rutherford scattering using an optical model code, JIB-3.¹² The results of these calculations showed that there was less than 1% deviation from Rutherford scattering for all the α scattering measurements, while the proton scattering results for Ca deviated by 11%. The Ni-foil thickness indicated by the α -particle measurement was $1.2 \pm 0.1 \times 10^{-5}$ cm.

The x rays ranging in energy from 3.7 to 7.5 keV exited the target chamber at 90° relative to the beam through a 0.0015-in. Mylar-foil window, and after traversing an air path of about 1.5 in. were detected in a gas proportional counter [Krypton (90%) - Methane (10%) at 1 atm] with a 0.010-in. Be window. The resolution at full width half-maximum (FWHM) for 5-keV x rays was 1 keV. The over-all detection efficiency of these x rays for this detector ranged from 65 to 77%. Air absorption (2.4–33.4%) was corrected for by mea-

suring the attenuation of each characteristic x ray for different air paths and extrapolating to zero air path. Attenuation in the Mylar foil (0.1–23.4%) was also measured directly by inserting a portion of this foil between the detector and the chamber window.

Pulses from the proportional counter were amplified and then fed to an ADC used with the on-line Honeywell DDP 224 computer. These pulses were also fed to a single-channel analyzer which was set to trigger on all pulses corresponding to x rays with energies ≥ 0.5 KeV. This permitted a check on total detector counting rate which was usually 10^3 sec^{-1} or less. A pulser was connected to the test input on the preamplifier to check the electronics and to provide a measure of the electronic deadtime losses. These were kept less than 10%, except at the highest bombarding energies where they were less than 25%. The pulser was calibrated with an ^{241}Am source and used to check the identification of x-ray photopeaks in the spectra.

Beam-current integration was used to provide normalization between points. The Faraday cup used to stop the beam was connected to a current integrator which produced a digital output. This digital output was fed to a master scaler which turned off the pulser scaler, the total-detector-counts scaler, and the ADC, after collecting a predetermined amount of charge, typically 0.06–2 μC . The integrator was checked with a precisely known current source to be accurate to better than 1%.

The effect of beam-associated electrons striking the target or being collected in the Faraday cup was checked by magnetically deflecting these electrons prior to their striking the target and with electron suppression prior to their being collected in the Faraday cup. In both cases the effect was less than 1%.

The use of thin targets (the $90\text{-}\mu\text{g}/\text{cm}^2$ Ni foil was the thickest) made some effort necessary to reduce the background in the region of the photopeak. The incident beam was first tightly focused on a quartz viewscreen about 60 cm upstream of the target and then passed through a $\frac{3}{32}$ -in. tantalum collimator about 15 cm upstream of the target. The x-ray detector could not see x rays arising from the scattered beam hitting the target ring owing to the placement of two collimators between the target and the Mylar window; however, background from fluorescence x rays, bremsstrahlung, and neutrons arising from the beam striking the forward collimator were still noticeable, particularly at beam energies above 10 MeV. Typical spectra for Ca, Ti, and Ni are shown in Figs. 2–4.

Photopeak intensities were extracted from the spectra by subtracting a straight-line background from under the photopeak and then summing over the area of the photopeak.

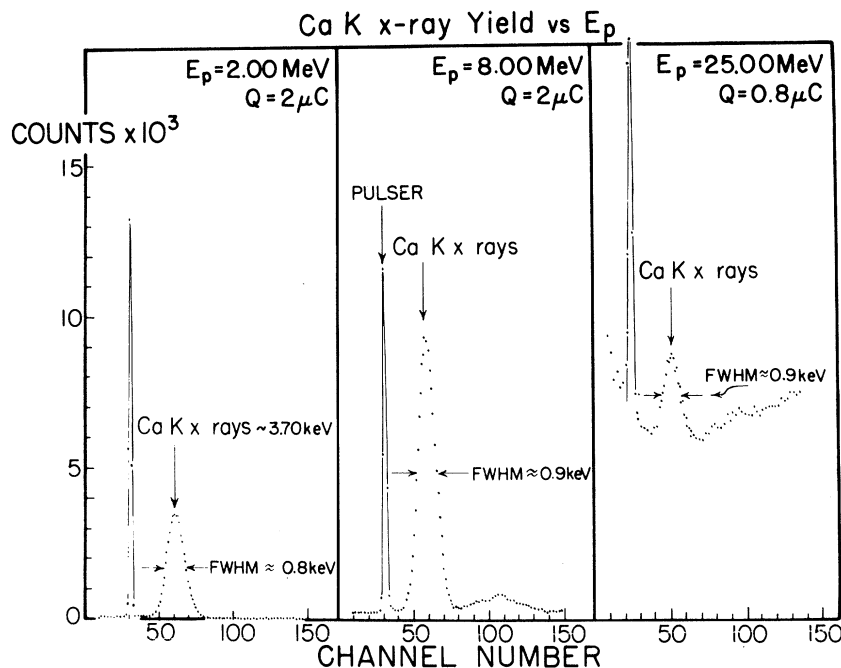


FIG. 2. Pulse-height spectra arising from Ca K x rays at $E_p=2, 8,$ and 25 MeV.

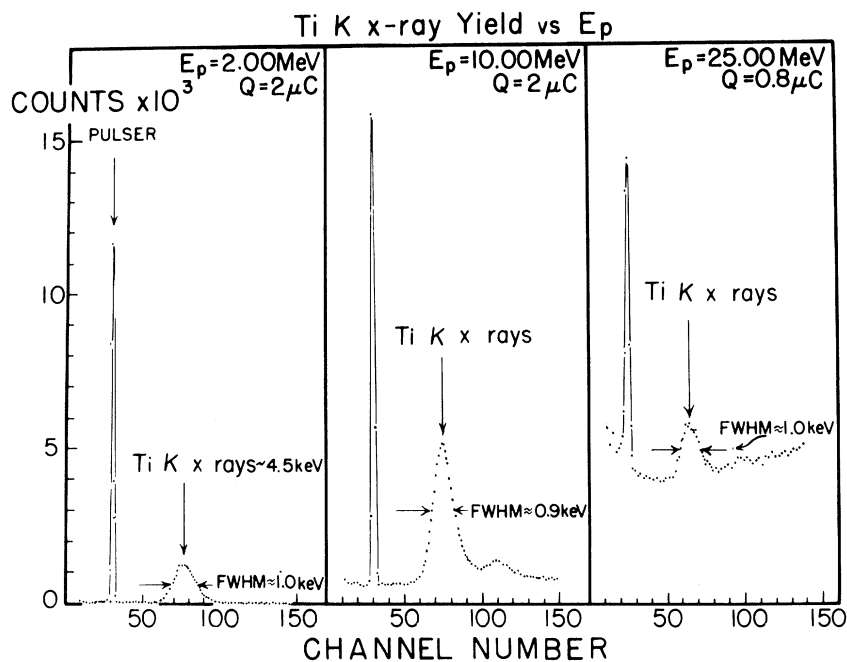


FIG. 3. Pulse-height spectra arising from Ti K x rays at $E_p=2, 10,$ and 25 MeV.

III. RESULTS AND DISCUSSION

Table I gives the observed K x-ray yields which were calculated from the formula

$$Y_K = N_{\text{obs}} / A \epsilon_{\text{ctr}} Q t \Omega, \tag{1}$$

where Y is the x rays per proton per sr per atom/cm². N_{obs} is the counts in the photo peak. The factor A is the correction for attenuation of the

x-ray flux by the Mylar window, air path, and beryllium window, and ϵ_{ctr} is the efficiency of the counter. Q is the number of protons incident on the target; t is the target thickness in atoms/cm². Ω is the solid angle subtended by the counter. This formula assumes that the K x rays are emitted isotropically. This assumption is reasonable since, for K x rays, $l=0$ electrons are ejected. It has been checked experimentally by Merzbacher and Lewis³ and found to be valid for L x rays from gold.

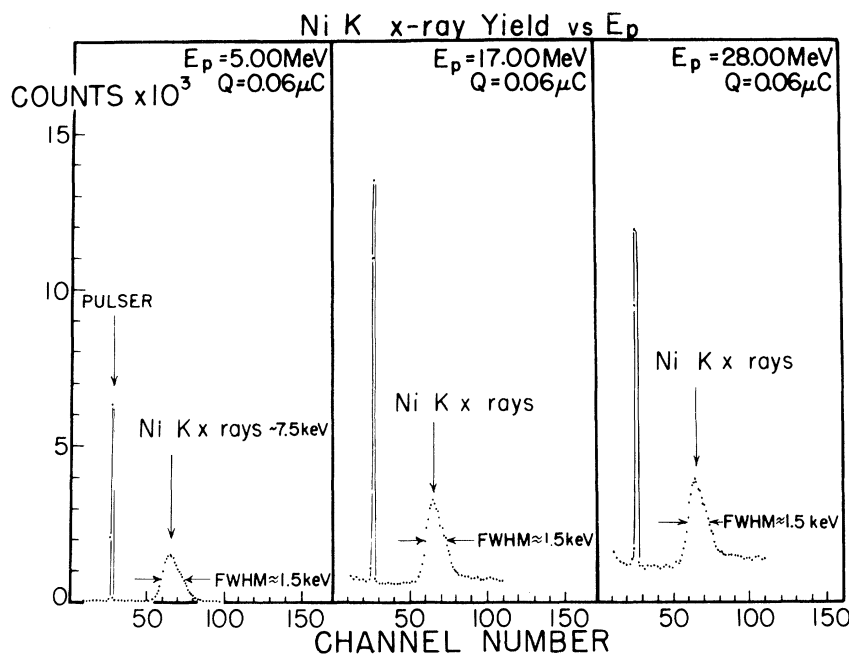


FIG. 4. Pulse-height spectra arising from Ni K x rays at $E_p = 5$, 17, and 28 MeV.

The quoted errors for the experimental results listed in Table I are derived from (i) the effect of choice of background to be subtracted and statistical variations in photopeak intensity; (ii) uncertainties in the corrections for x-ray absorption in the Mylar window (1.0–1.3%), air path (0.5–2.0%), Be window (1.1–1.5%), and proportional counter gas (0.1–1.4%); and (iii), most important, uncertainty in measured target thickness (10.0–11.8%). These were treated as random errors and combined in the usual manner.

Table I also gives the cross section for K -shell ionization, which is simply related to K x-ray production; i. e.,

$$\sigma_K = 4\pi\omega_K^{-1}Y_K, \quad (2)$$

where ω_K is the correction factor for the competing Auger effect. The correction for the Auger effect is more than twice as large as the combined correction for absorption and efficiency effects. It is also the least accurate correction. There do not seem to be accepted experimental values of ω_K for Ca, Ti, and Ni (see, e.g., the article¹³ by R. W. Fink *et al.* for discussion about values of ω_K for these and other atoms), hence the values of ω_K used in the present work were calculated from the semiempirical formula

$$\omega_K(1 - \omega_K)^{-1} = (-A + BZ - CZ^3)^4 \quad (3)$$

considered reliable for $Z > 17$. Values for the empirical constants, $A = 0.064$, $B = 0.034$, and $C = 1.03 \times 10^{-6}$, are those of Hagedoorn and

Wapstra.¹⁴ The values of ω_K calculated from (3) were $\omega_K = 0.120$ for Ca, $\omega_K = 0.170$ for Ti, and $\omega_K = 0.359$ for Ni, all with an uncertainty of ± 0.005 . However, recent measurements by Taylor and Merritt¹⁵ for V, Cr, and Cu indicate that the values of ω_K calculated from (3) for these atoms may be low by as much as 25%. This, of course, would reduce values of σ_K quoted in Table I by as much as 25%, if their measurements are confirmed.

The experimental values of σ_K listed in Table I are plotted versus E_p for Ca, Ti, and Ni in Figs. 5–7. These figures also contain theoretical curves for σ_K . They were derived from a paper by Khandelwal, Choi, and Merzbacher.¹⁶ Values for the screening constant θ_K of 0.76, 0.77, and 0.79 for Ca, Ti and Ni, respectively, were taken from Walske,¹⁷ where

$$\theta_K = I_K / (Z_K^2 \text{ Ry}). \quad (4)$$

I_K is the K -shell ionization energy, and Z_K is the effective charge seen by the K -shell electrons. Theoretical values for the K -shell ionization cross section were calculated from the expression

$$\sigma_K = (8\pi z^2 a_0^2 / Z_K^4) (f_K / \eta_K), \quad (5)$$

where z is the charge of the beam projectile, and a_0 is the Bohr radius. The quantities f_K , which are related to the form factor and which must be calculated numerically, are tabulated in Ref. 16; η_K is related to the beam energy E by the expression

TABLE I. K -shell ionization cross sections and K x-ray yields.

E_p (MeV)	Ca		Ti		Ni	
	σ_K^a (barns)	$\sigma_{K/4\pi\omega_K^{-1}}$ (b/sr) ^d	σ_K^b (barns)	$\sigma_{K/4\pi\omega_K^{-1}}$ (b/sr) ^d	σ_K^c (barns)	$\sigma_{K/4\pi\omega_K^{-1}}$ (b/sr) ^d
2.0	1950 ±250	18.6 ±2.4	1300 ±160	17.6 ±2.2		
3.0	3290 ±420	31.4 ±4.0	2170 ±270	29.4 ±3.7		
4.0	4120 ±530	39.3 ±5.1	2880 ±360	38.9 ±4.9		
5.0	4800 ±610	45.8 ±5.8	3250 ±410	44.0 ±5.6	820 ±90	23.4 ±2.6
6.0	4940 ±630	47.2 ±6.0	3680 ±460	49.8 ±6.2		
7.0	5270 ±670	50.3 ±6.4	3900 ±490	52.8 ±6.6		
8.0	5240 ±670	50.0 ±6.4	4090 ±510	55.3 ±6.9	1140 ±130	32.6 ±3.7
9.0	5290 ±710	50.5 ±6.8	4100 ±520	55.5 ±7.0		
10.0	5100 ±680	48.7 ±6.5	4220 ±530	57.1 ±7.2		
11.0	5140 ±690	49.1 ±6.6	4070 ±530	55.1 ±7.2	1330 ±150	38.0 ±4.3
12.0	5150 ±690	49.2 ±6.6	3970 ±520	53.7 ±7.0		
13.0	5040 ±670	48.1 ±6.4	3790 ±490	51.3 ±6.6		
14.0					1460 ±160	41.7 ±4.6
16.5	4490 ±600	42.9 ±5.7	4080 ±530	55.2 ±7.2		
17.0					1440 ±170	41.1 ±4.9
20.0	4550 ±660	43.5 ±6.3	3600 ±490	48.7 ±6.6	1520 ±200	43.4 ±5.7
24.0					1420 ±190	40.6 ±5.4
25.0	3740 ±550	35.7 ±5.3	3390 ±460	45.9 ±6.2		
28.0					1410 ±190	40.3 ±5.4

^aFor Ca: $\omega_K=0.120$.^bFor Ti: $\omega_K=0.170$.^cFor Ni: $\omega_K=0.359$.^dUnits are equivalent to quanta/proton sr (nucleus/cm²).

$$\eta_K = mE/M(Z_K^{-2} \text{ Ry}),$$

(6)

where m and M are the mass of the electron and beam particle, respectively. Also shown in Figs.

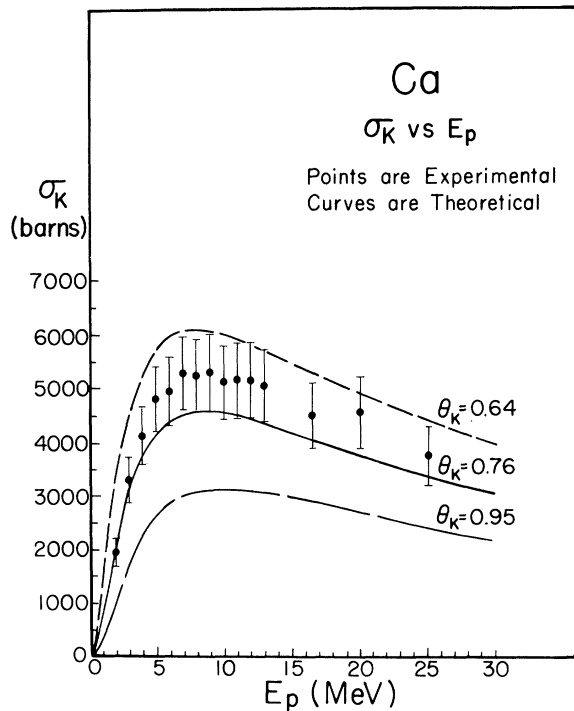


FIG. 5. Absolute K -shell ionization cross section (σ_K) for Ca compared to theory (Ref. 16) for various choices of θ_K . A realistic value (Ref. 17) of θ_K is 0.76.

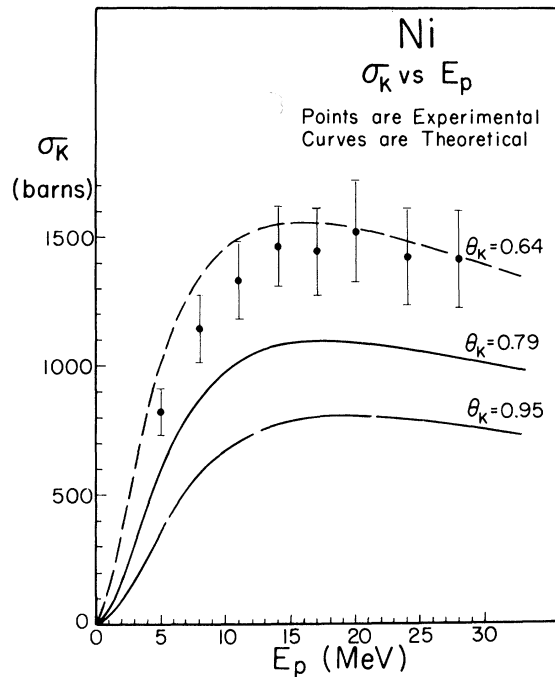


FIG. 7. Absolute K -shell ionization cross section (σ_K) for Ni compared to theory (Ref. 16) for various choices of θ_K . A realistic value (Ref. 17) of θ_K is 0.79.

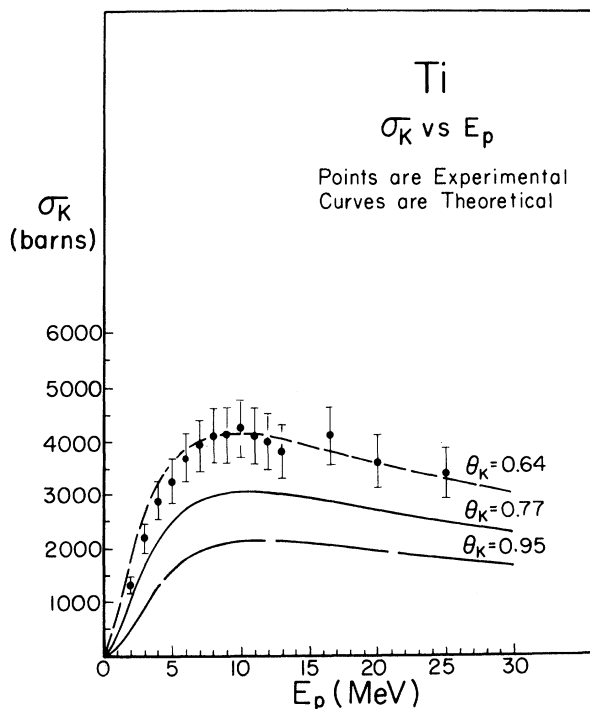


FIG. 6. Absolute K -shell ionization cross section (σ_K) for Ti compared to theory (Ref. 16) for various choices of θ_K . A realistic value (Ref. 17) of θ_K is 0.77.

5-7 are theoretical curves for $\theta_K = 0.64$ and 0.95 , the extreme value for the screening constant contained in Ref. 16.

It can be seen from Figs. 5-7 that (i) the maxima in the experimental K -shell ionization cross sections fall quite close to the values of 8.5, 10.4, and 16.6 MeV for Ca, Ti, and Ni estimated from the theoretical curves in Fig. 4 of Merzbacher and Lewis, (ii) the relative cross sections follow the trend of theory quite closely, except at lower energies where they tend to lie somewhat low, and (iii) if the values of θ_K taken from Walske are chosen, then the experimental points (within error) always lie on or above the theoretical curve, i.e., in the region of lower values for θ_K .

Among the possible reasons for the difference between theory and experiment are (a) inaccurate values of the fluorescence yields ω_K , (b) imperfect inclusion of electron screening effects in the theory, (c) omission of distortion of the proton wave function by nuclear Coulomb repulsion, (d) polarization of the electron orbits by the incoming proton, and (e) neglect of relativistic effects in describing the electron motion.

For purposes of comparison, Fig. 8 shows our data plotted on a "universal" curve with ordinate $\theta_K Z_K^4 \sigma_K$ and abscissa η_K / θ_K^2 along with those of Khan *et al.* for carbon and de Heer *et al.*¹⁸ for helium. It should be noted that the theoretical

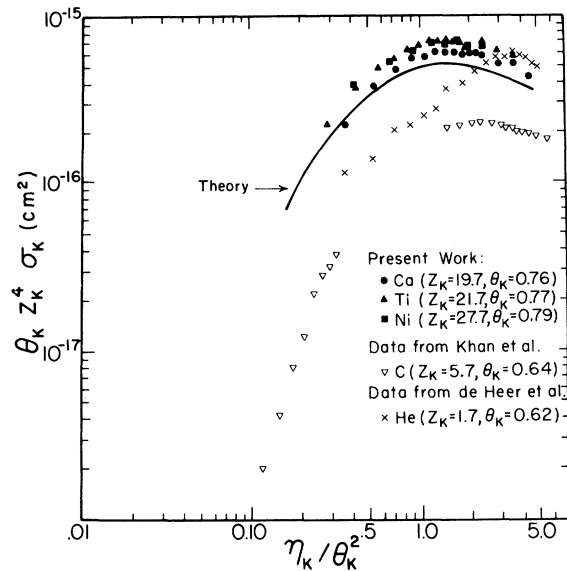


FIG. 8. Universal curve: present work for Ca, Ti, and Ni and the data of Khan *et al.* (Ref. 6) for carbon with revised stopping powers from J. H. Ormrod and H. E. Duckworth, *Can. J. Phys.* **41**, 1424 (1963). The He data is from de Heer *et al.* (Ref. 18).

curve¹⁶ is for Ni; somewhat different curves would be obtained for other atomic numbers.

The data of de Heer *et al.* are independent of fluorescence yield since they detected charged particles instead of x rays, which is an advantage since the fluorescence-yield correction is very large for low Z atoms and not well known. This may explain why the carbon data lie so low com-

pared to our data and the helium data.

The present work using thin targets overlaps the thick-target work of Merzbacher and Lewis³ for Ti at beam energies of 2 and 3 MeV. Their values for the absolute cross section σ_K are 1500 and 2720 b at $E_p = 2$ and 3 MeV, respectively, while those for the present work (Table I) are 1300 ± 160 and 2170 ± 220 b at the same energies. In view of the difficulties in extracting absolute cross sections in both experiments, we feel that this constitutes reasonable agreement.

In conclusion, our results indicate that the experimental K -shell ionization cross sections for Ca, Ti, and Ni are in general agreement with the theoretical predictions of Ref. 3, although for the chosen values of screening constant θ_K , the experimental results fall above the theoretical results. Also there is a tendency for the low-energy points to lie lower relative to the theoretical predictions than the high-energy points. The predicted Z dependence of both the magnitude of σ_K and the variation with proton energy of the maximum in σ_K was in agreement with the results of this work.

ACKNOWLEDGMENTS

We are grateful to Dr. E. Merzbacher for drawing our attention to this problem, for encouragement, and for many helpful discussions. We wish to thank Dr. G. S. Khandelwal for helpful discussions concerning theoretical aspects. We are indebted to Dr. E. G. Bilpuch for the loan of the ⁴⁴Ca and Ti targets; to Dr. F. G. C. Perey for the optical-model code JIB-3; and to Dr. Dietrich Schroerer for the loan of the proportional counter.

*Work done under the auspices of the U. S. Atomic Energy Commission.

¹J. Chadwick, *Phil. Mag.* **24**, 594 (1912).

²H. W. Lewis, B. E. Simmons, and E. Merzbacher, *Phys. Rev.* **91**, 943 (1953).

³E. Merzbacher and H. W. Lewis, *Encyclopedia of Physics* (Springer-Verlag, Berlin, 1958), Vol. 34, p. 166.

⁴W. Henneberg, *Z. Physik* **86**, 592 (1933).

⁵R. R. Hart, F. W. Reuter, III, H. P. Smith, Jr., and J. M. Khan, *Phys. Rev.* **179**, 4 (1969).

⁶J. M. Khan, D. L. Potter, and R. D. Worley, *Phys. Rev.* **139**, A1735 (1965).

⁷See K. L. Bell and A. E. Kingston, *J. Phys.* **B2**, 653 (1969) for experimental references.

⁸*Studies in Penetration of Charged Particles in Matter*, edited by U. Fano (Printing and Publishing Office, National Academy of Sciences - National Research Council, Washington 25, D. C., 1964), Publication No. 1133.

⁹H. W. Newson, F. O. Purser, N. R. Roberson, E. G.

Bilpuch, R. L. Walter, and E. J. Ludwig, *Bull. Am. Phys. Soc.* **14**, 533 (1969).

¹⁰H. Coleman, M. S. thesis, Duke University, 1968 (unpublished).

¹¹Supplied by the Chromium Corporation of America, Waterbury, Conn.

¹²Provided through the courtesy of F. G. C. Perey.

¹³R. W. Fink, R. C. Jopson, H. Mark, and C. R. Swift, *Rev. Mod. Phys.* **38**, 513 (1966).

¹⁴H. L. Hagedoorn and A. H. Wapstra, *Nucl. Phys.* **15**, 146 (1960).

¹⁵J. G. V. Taylor and J. S. Merritt, *Proceedings of Conference in Atomic Electrons in Nuclear Transformations*, (Nuclear Energy Information Center, Warsaw, 1963), Vol. III, p. 465.

¹⁶G. S. Khandelwal, B. H. Choi, and E. Merzbacher, *Atomic Data* **1**, 103 (1969).

¹⁷M. C. Walske, *Phys. Rev.* **101**, 940 (1956).

¹⁸F. J. de Heer, J. Schutten, and H. Moustafa, *Physica*, **32**, 1766 (1966).